UPPSALA UNIVERSITET

Convective eddy motions in rapid transitions to near-surface stable stratification: a large-eddy simulation study

Erik Nilsson

Department of Earth Sciences, Uppsala University

Courtesy of many collaboraters: Nina Svensson, Anna Rutgersson, Marcus Wallin, Erik Sahlée, Hans Bergström, Gunnar Bergström, Adam Dingwell, Larry Mahrt and many more…

Convective eddy motions in rapid transitions to near-surface stable stratification

Background for this work:

- ICOS marine station Östergarnsholm on a small island in the Baltic Sea
- Semi-continuous measurements since 1995 to collect various atmospheric measurements both means and turbulence as well as water measurements
- Some studies about the representativity of the site have been done but more are being conducted
- Also working in various wave energy projects for the Baltic Sea which was useful also for the current work

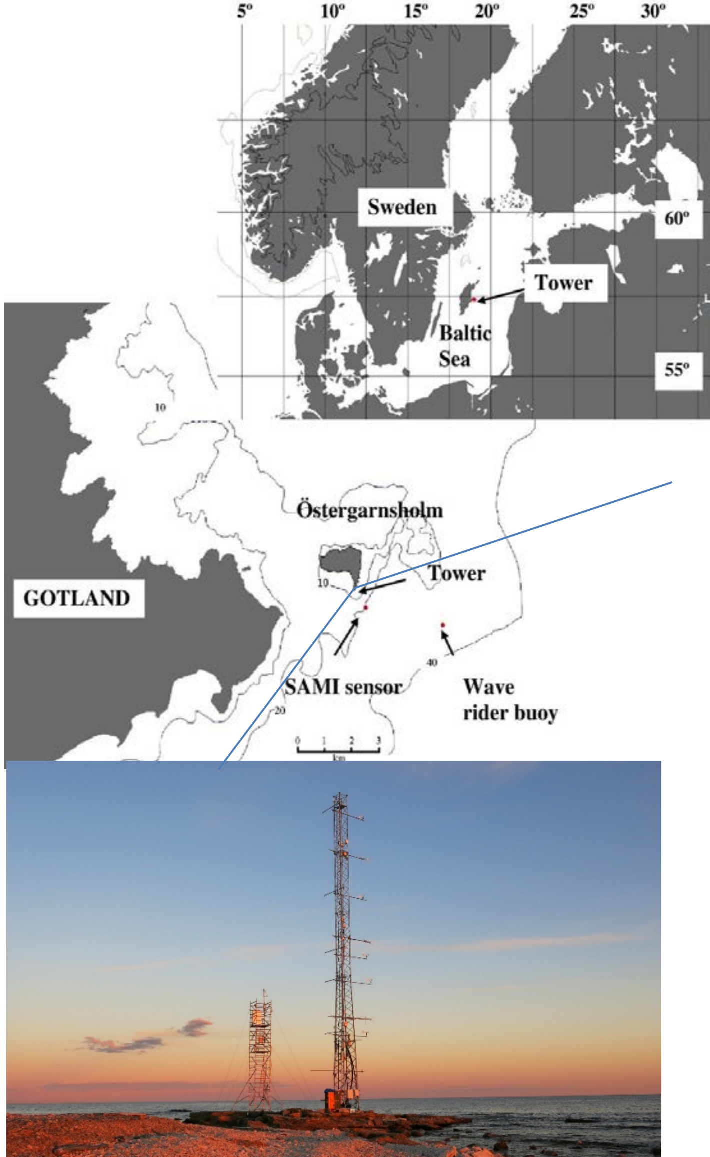

Long term measurements to analyze distributions of winds, stability and fluxes

1. Measurements and modeling is used to obtain information about typical range of variations at the site

2. From this we choose LES settings

3. Idealized simulations of rapid transitions from rough to smooth surface and from convective to stable conditions using the NCAR LES model

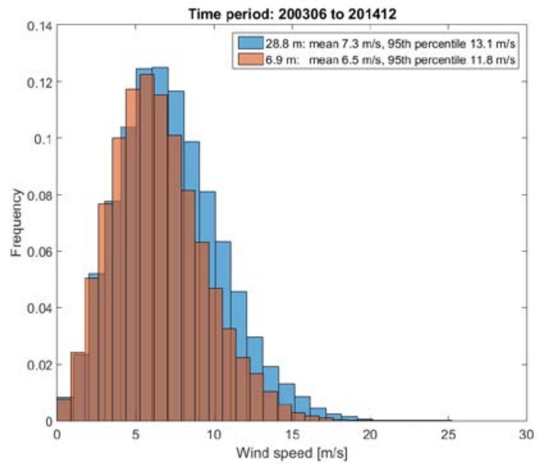

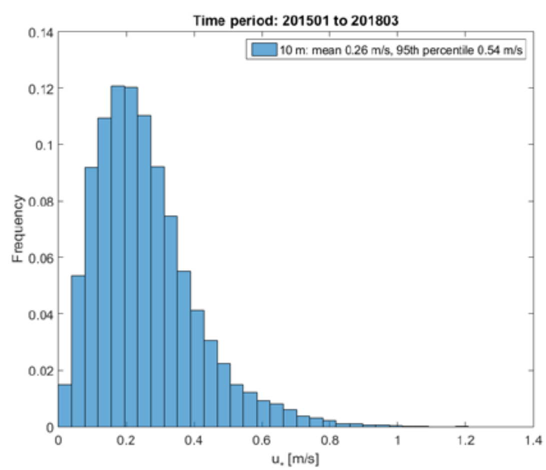

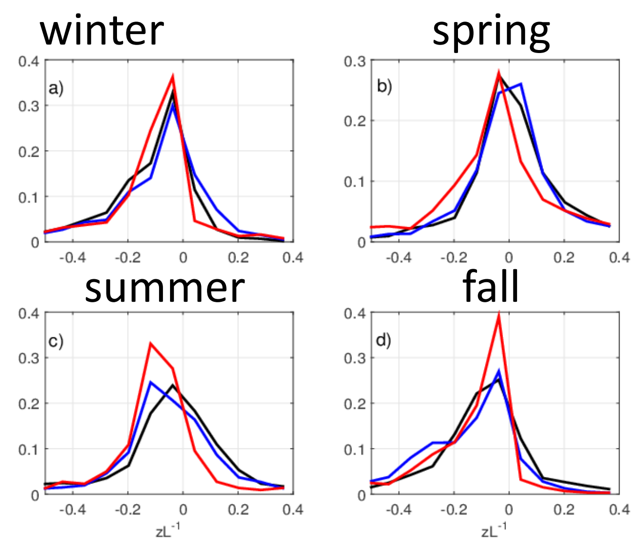

Black open sea sector

Blue coastal sector

Red mixed land-sea sector

Rutgersson et al. (2018) submitted

Probability of unstable and close to neutral unstable conditions is large (too large?) compared to expected climatology for the Baltic Sea

Influence from land (Gotland)?

UPPSALA UNIVERSITET

WRF modeling and a third generation wave model (WAM) to study spatial variation

- In coastal transitions change in roughness can be important

1. High resolution winds were obtained for one year (201107-201206) by dynamical downscaling using the WRF model (9, 3 , 1 km horizontal resolution) for the Baltic Sea

2. The winds were then used as input for the wave model WAM to predict the wave field that influence the frictional stress at the surface

3. Spatial variation in friction velocity and surface roughness were assessed

4. A set of z_0 values ranging from typical (median) to less typical (95th percentile) for sea conditions were chosen and used in idealized large-eddy simulations of rapid transitions

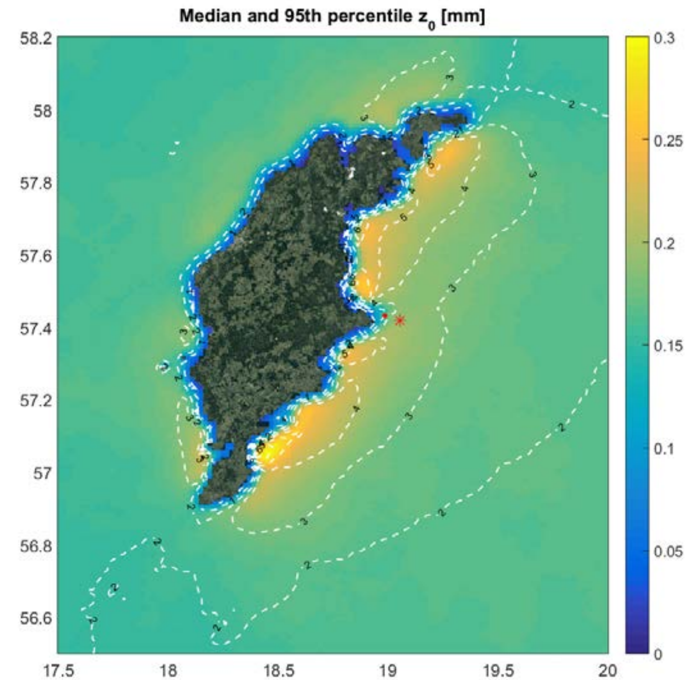

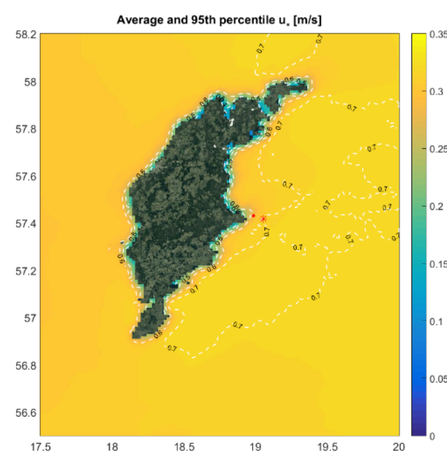

Idealized large-eddy simulations of rapid transitions

Initialized with the same convective turbulence for each simulation with same U_g

land	sea
U_g = (5), 10, 15 m/s	U_g kept constant
Q_* ~ 0.01 Km/s	Q_* ~ 0.01, 0.0, -0.005, -0.01, -0.02 Km/s
z_0 ~ 20 mm	z_0 ~ 0.2, 0.64, 2.0, 6.4, 20 mm

Varying the surface heat flux and surface roughness systematically: 13 simulations for each geostrophic wind speed

Each simulation: 90 minutes, some statistics saved every 1 s, flow field every 10 s

Setup details similar as in: Nilsson et al. (2012)

We study the evolution of flow with regards to frictional stresses, TKE and also different definitions of z_i and S-shaped heat flux profiles

land	sea
u_* ~ 0.36 to 0.48 m/s	u_* ~ 0.13 to 0.43 m/s
z_i ~ 500 to 600 m	z_i definition during transitions?
z_i/L ~ -0.8 to -1.6	

Idealized large-eddy simulations of rapid transitions

The simulations include several types of flow features such as:

- Convective turbulence decaying as stratification changes (approx. 1 eddy turn-over time scale)
- Horizontal boundary layer rolls that survives a couple large eddy turnover time scales
- Near surface stable boundary layer growing (depends on turbulence level, mainly controlled by shear production)
- Entrainment zone weakening (but remains also after many eddy turn-over time scales)
- Flow acceleration sometimes forming conditions for low-level jets in low wind (especially ageostrophic component, inertial oscillation?)

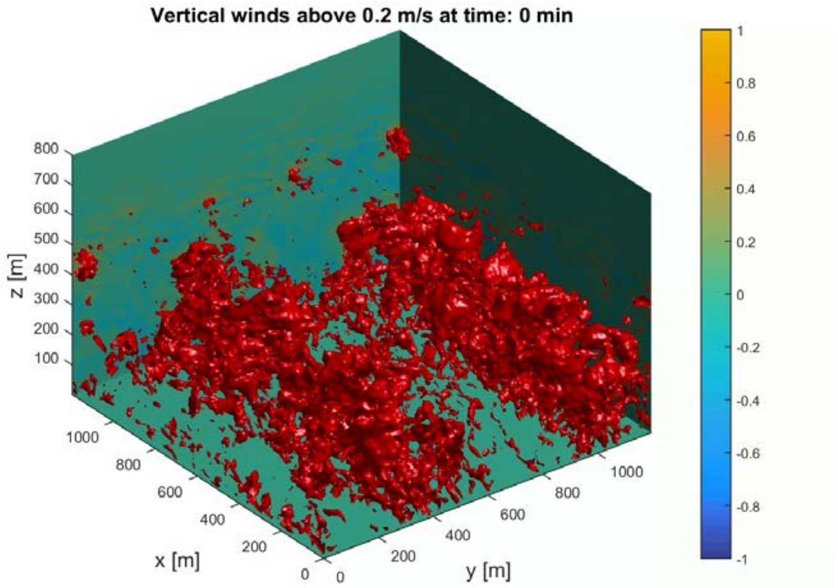

- Friction decreasing as turbulence decays (different decay due to stratification or reduced surface roughness)

UPPSALA UNIVERSITET

TKE height dependence:
Yellow (no change in strat. or roughness)

Red (only reduced roughness)

Black (change to neutral)

Blue (change to stable)

Purple (change to stable and reduced roughness)

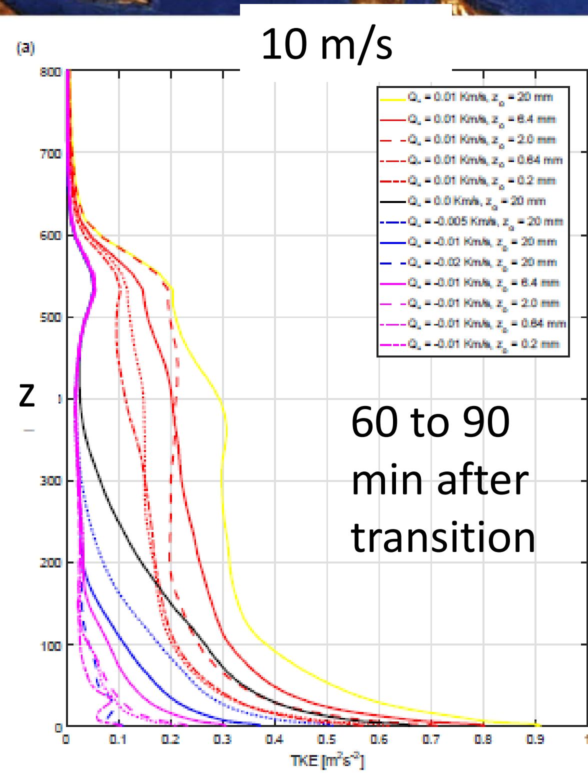

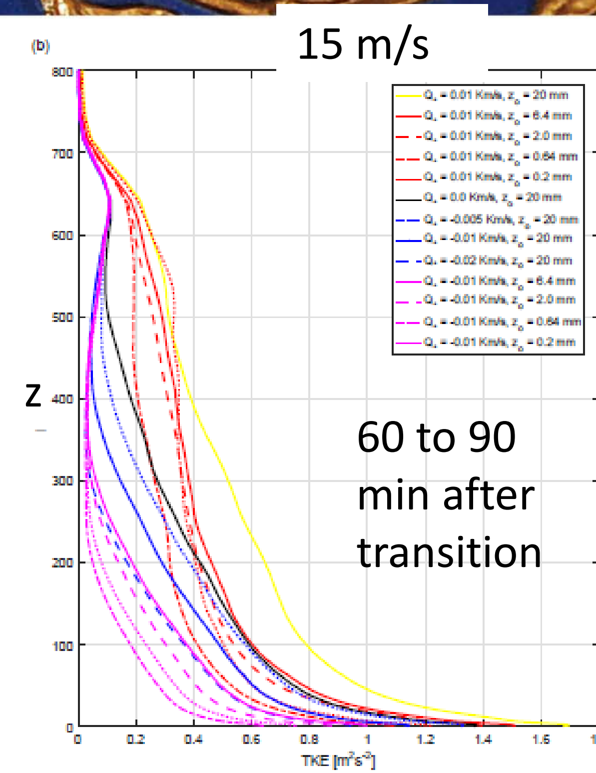

TKE time dependence (129 m):
Same development approx. 1 eddy turnover time scale because of last convective eddy motions

Afterwards a combination of smooth surface and stable stratification can nearly collapse turbulence completely

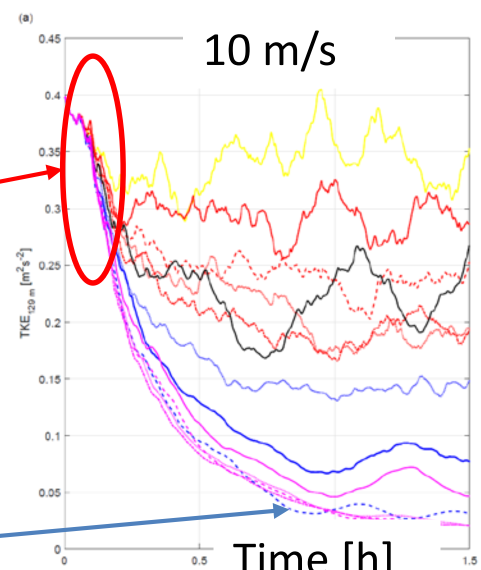

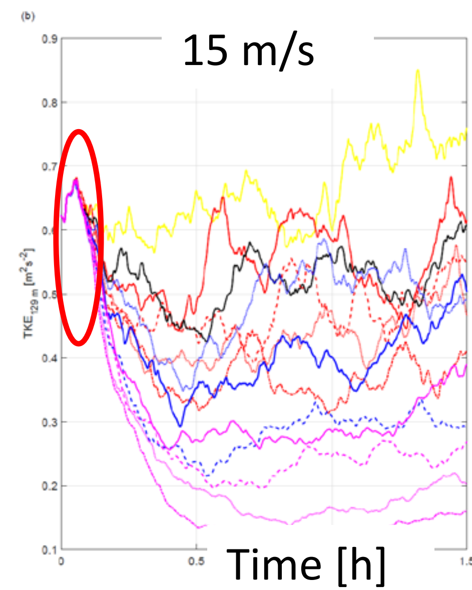

UPPSALA UNIVERSITET

Heat flux time dependence (129 m):
Positive values remain approx. 1 large eddy turnover time scale because of last convective eddy motions

Afterwards in stable stratification heat flux can get a ’back-lash’ period with stronger negative heat flux,
before settling at a equilibrium level or weak decreasing time trend.
Mahrt (2017) has found this also from field measurements on some sites (CASES-99)

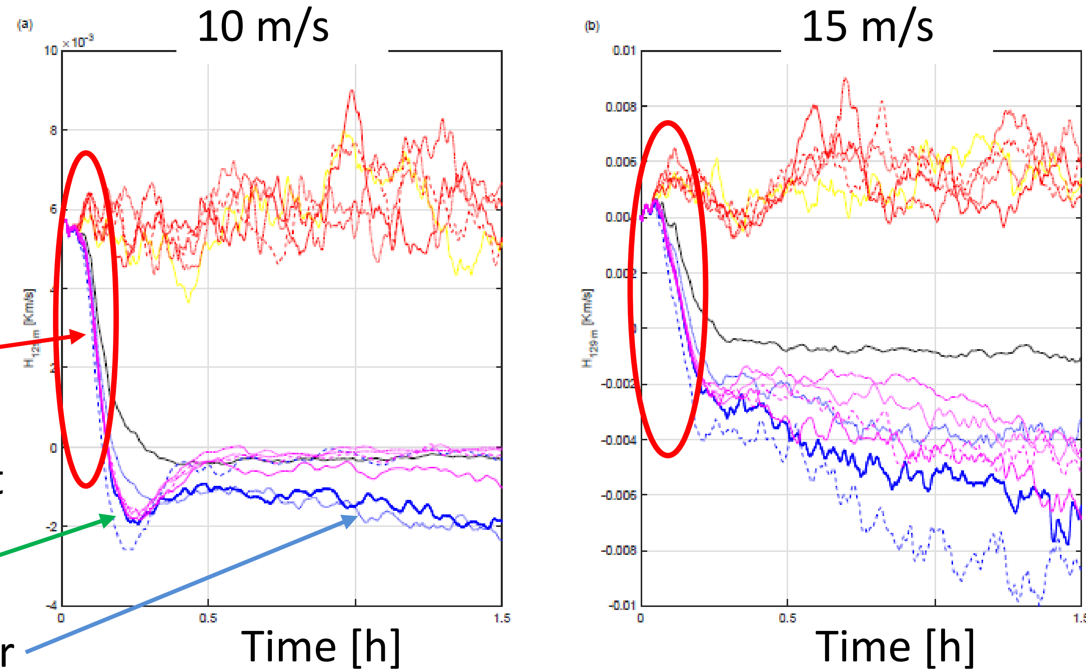

Heat flux height dependence:
In the last 30 min averaged profile: No positive heat flux for the stable cases.
Neutral and strong wind cases show some weak stable profile despite zero flux at surface

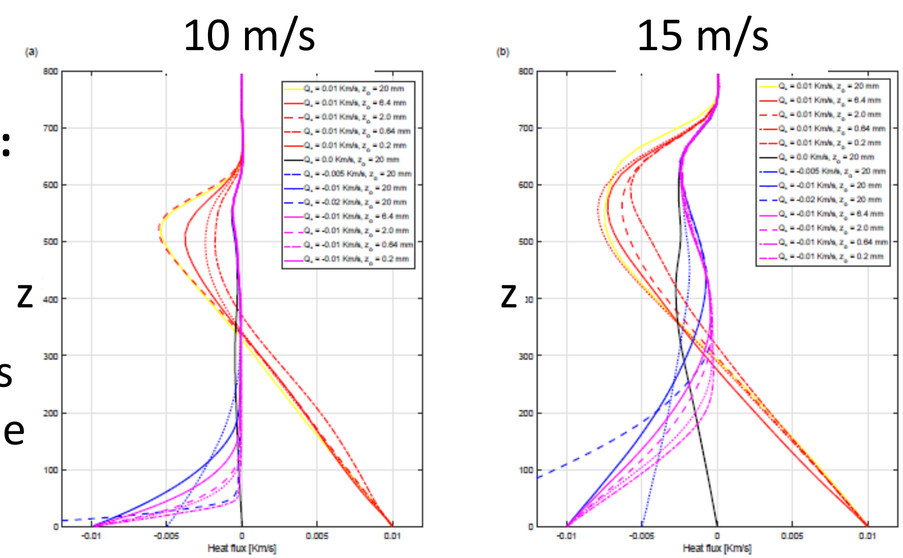

UPPSALA UNIVERSITET

Wind speed height dependence:

- Reduced surface roughness alone cause flow acceleration all heights
- Flow acceleration mostly in upper parts of boundary layer in transition to neutral and stable

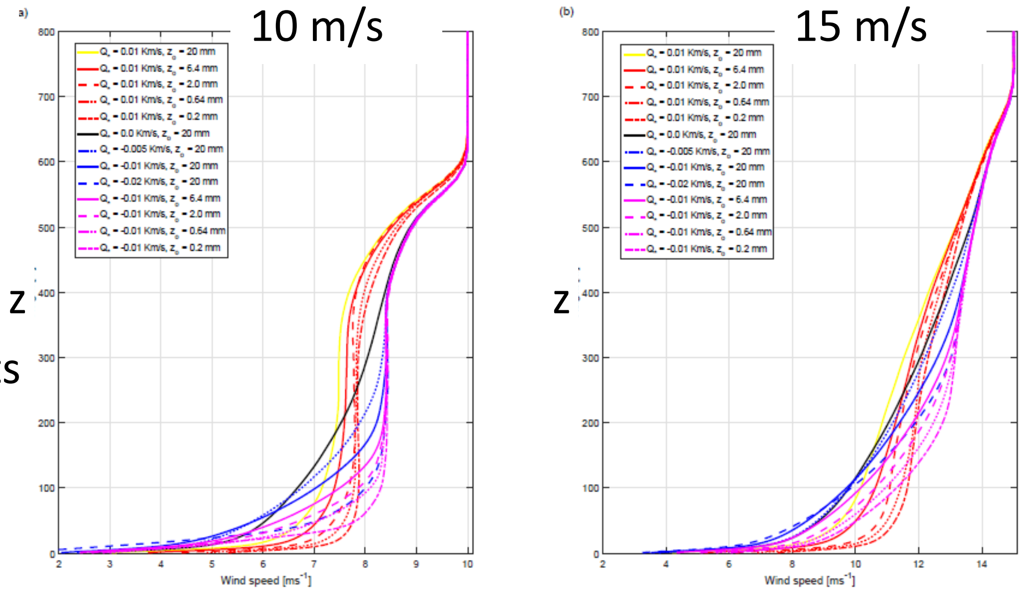

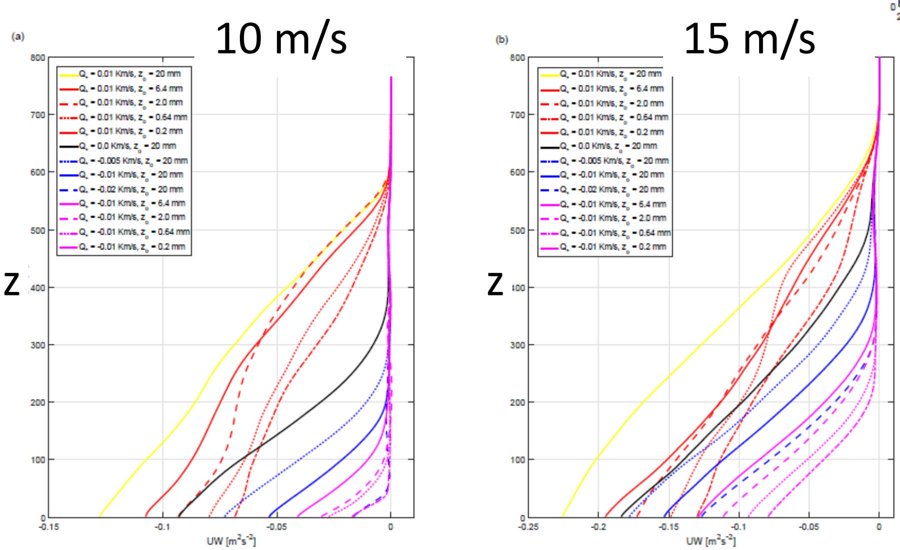

Streamwise kinematic momentum flux:

Nearly linear decay up to some height

In convective: CBL top independent of z_o

In stable: depends on stratification and z_0

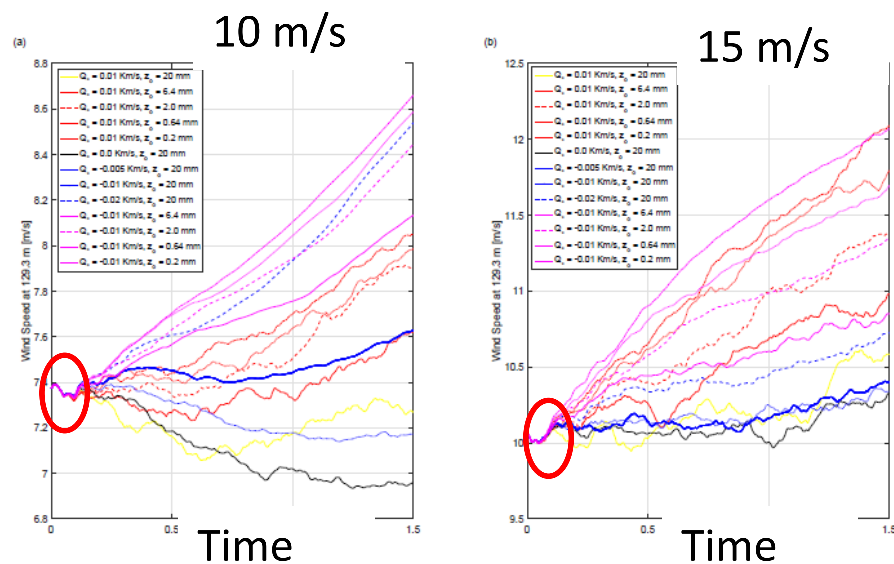

Timeseries: U_{129m} mostly increase but sometimes decrease in wind speed

UPPSALA UNIVERSITET

Tracking the development of four different types of boundary layer depths:

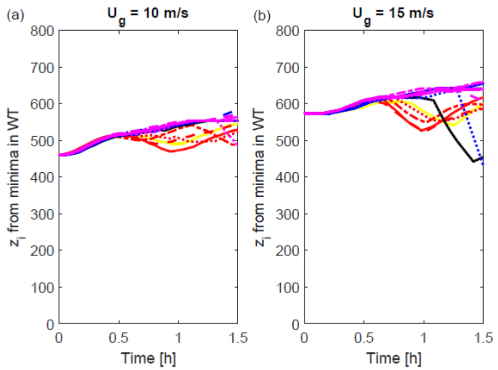

Figure 11. Development of a residual layer boundary layer depth determined from an elevated local minima of kinematic heat flux for the transitory period following 90 min after a rapid transition.

$z_{i(WT)}$

Good for tracking the old CBL entrainment zone

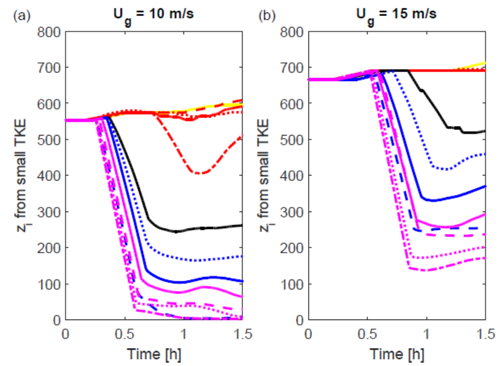

Figure 12. Decay of turbulent boundary layer depth determined from first height at which TKE falls below a threshold value is shown for the transitory period following 90 min after a rapid transition.

$z_{i(TKE)}$

Good for tracking the TKE decay (but can miss entrainment zone TKE)

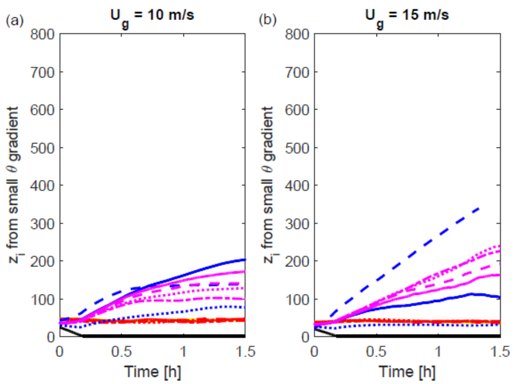

Figure 14. Development of a stable boundary layer depth determined from the first height at which the magnitude of the gradient of potential temperature is smaller than a threshold value. Different colored lines for the transitory period following 90 min after a rapid transition shows different cases.

$z_{i(d\theta/dz)}$

Good for tracking the growing near-surface BL or start of 'mixed layer profile'

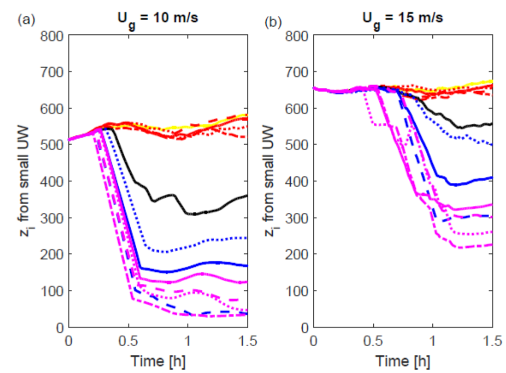

Figure 13. Development of a frictional boundary layer depth determined from the first height at which the magnitude of streamwise stress falls below a threshold value. Different colored lines for the transitory period following 90 min after a rapid transition shows different cases.

$z_{i(UW)}$

Similar as TKE criteria but less confusion because the stress is small in the EZ zone

UPPSALA UNIVERSITET

Example for two simulations:

Unstable case

Stable case

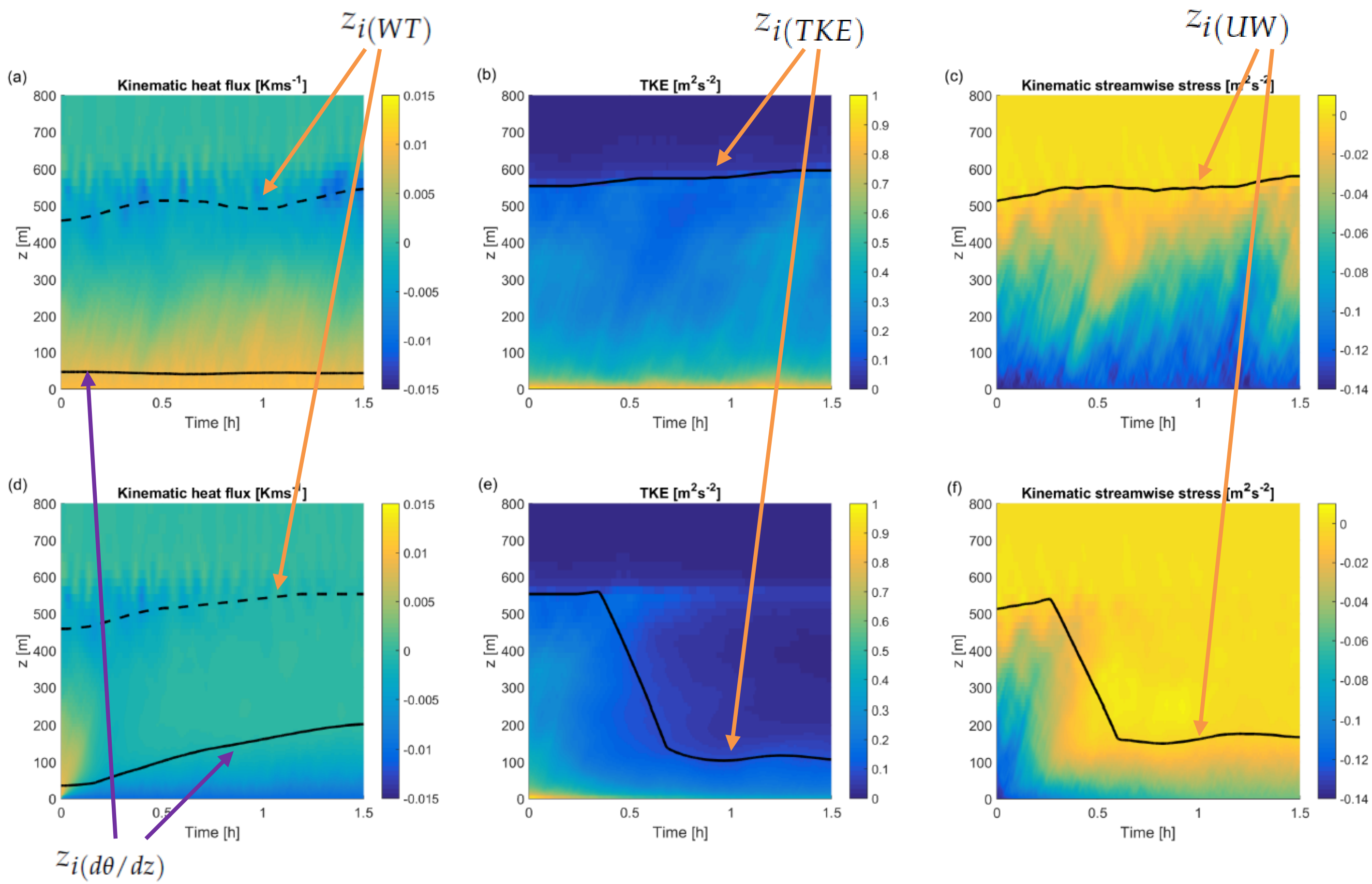

Figure 10. Development of kinematic heat flux (a and d), TKE (b and e) and streamwise kinematic stress (c and f) for two cases one with unstable (top) and one with stable near-surface stratification (bottom). Included are also black lines corresponding to four boundary layer depths defined from 10 min running mean values, see text for further explanation.

In rapid transitions the lingering positive heat flux causes an S-shape profile and the flux remains positive about 1 large-eddy turnover time scale (Sorbjan 1997, Niewstadt and Brost 1986) in middle of the positive flux layer

In surface layer the flux become negative sooner

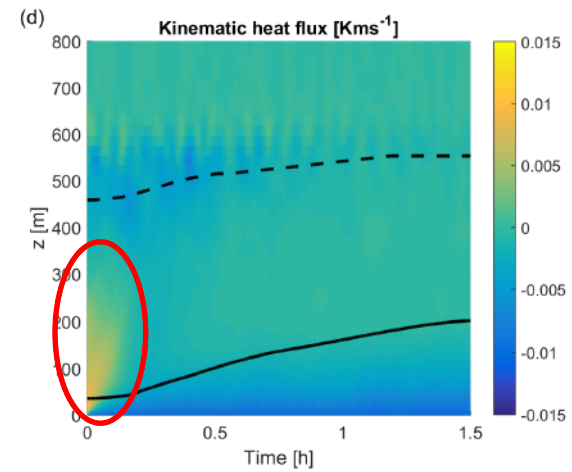

In transition to neutral the flux remains positive longer

Stronger stable stratification at the surface causes the time with positive flux to decrease

Little sensitivity to change in surface roughness (for the studied range)

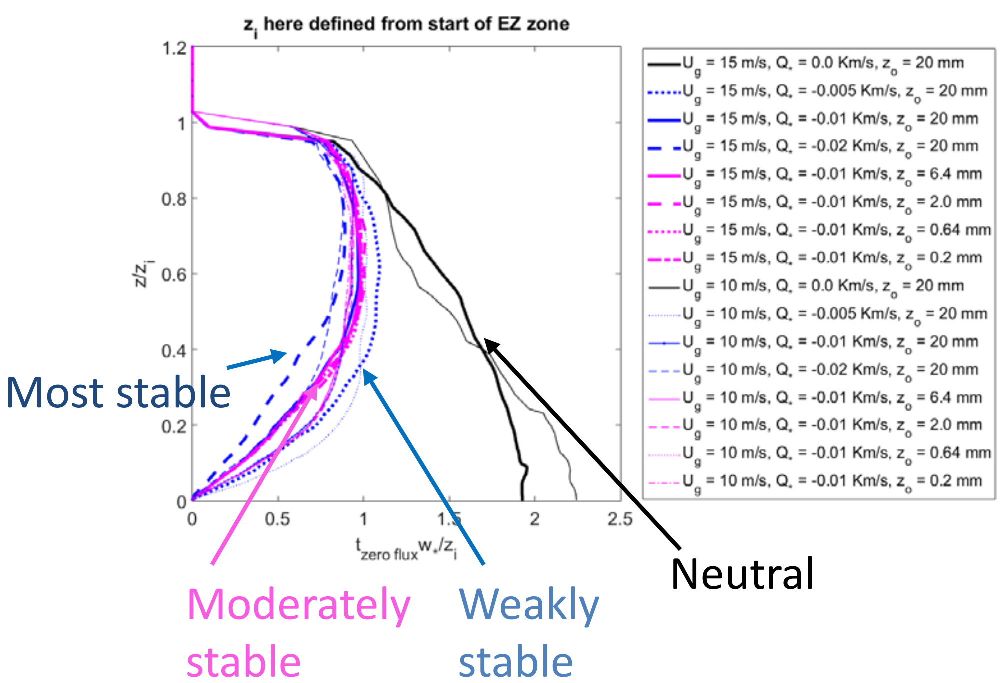

Returning to the question of the high probability of unstable and near-neutral conditions measured at Östergarnsholm

- For the highest tower level (29 m) at Östergarnsholm advection effects from larger than 3 km away can likely occur in situations of unstable stratification on the island of Gotland. Assuming typical median wind speeds (7 m/s) as approx. advection speed and typical z_i and stabilities
- For the lower tower turbulence levels (16, 10 m) the effects are reduced but should be further studied
- Choosing carefully wind direction sectors and using flux footprint models is important to evaluate representative sea conditions
- Influence from 10 to 30 min before each time period with wind direction from sea sectors should also be considered due to flow memory effects.
- Rapid wind directional shifts are quite common on the site and is now being studied by Larry Mahrt

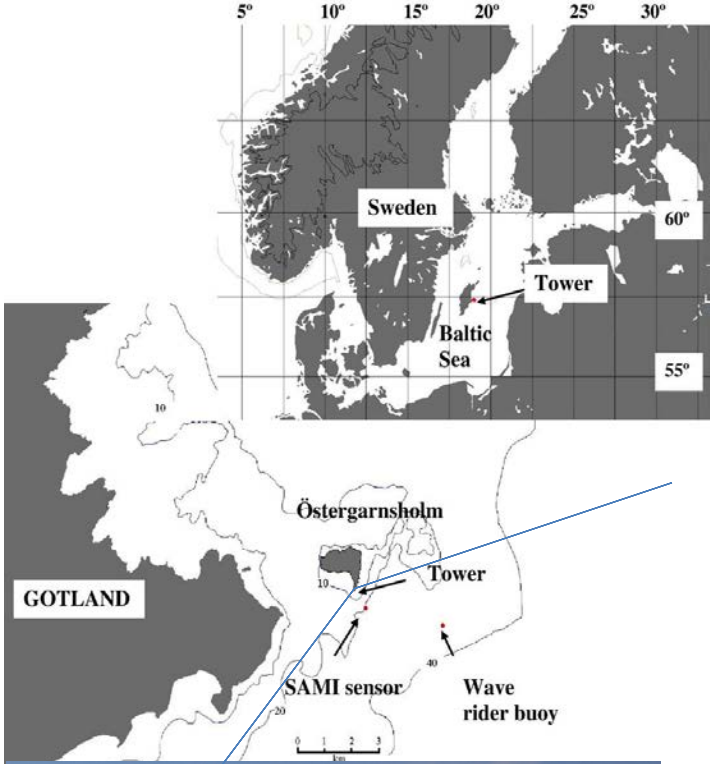

UPPSALA UNIVERSITET

Thank you for listening!

Photo: Stefan Osterwalder during the Gotland Hg campaign studying the flux of mercury from the Baltic Sea coastal zone

UPPSALA
UNIVERSITET

UPPSALA UNIVERSITET

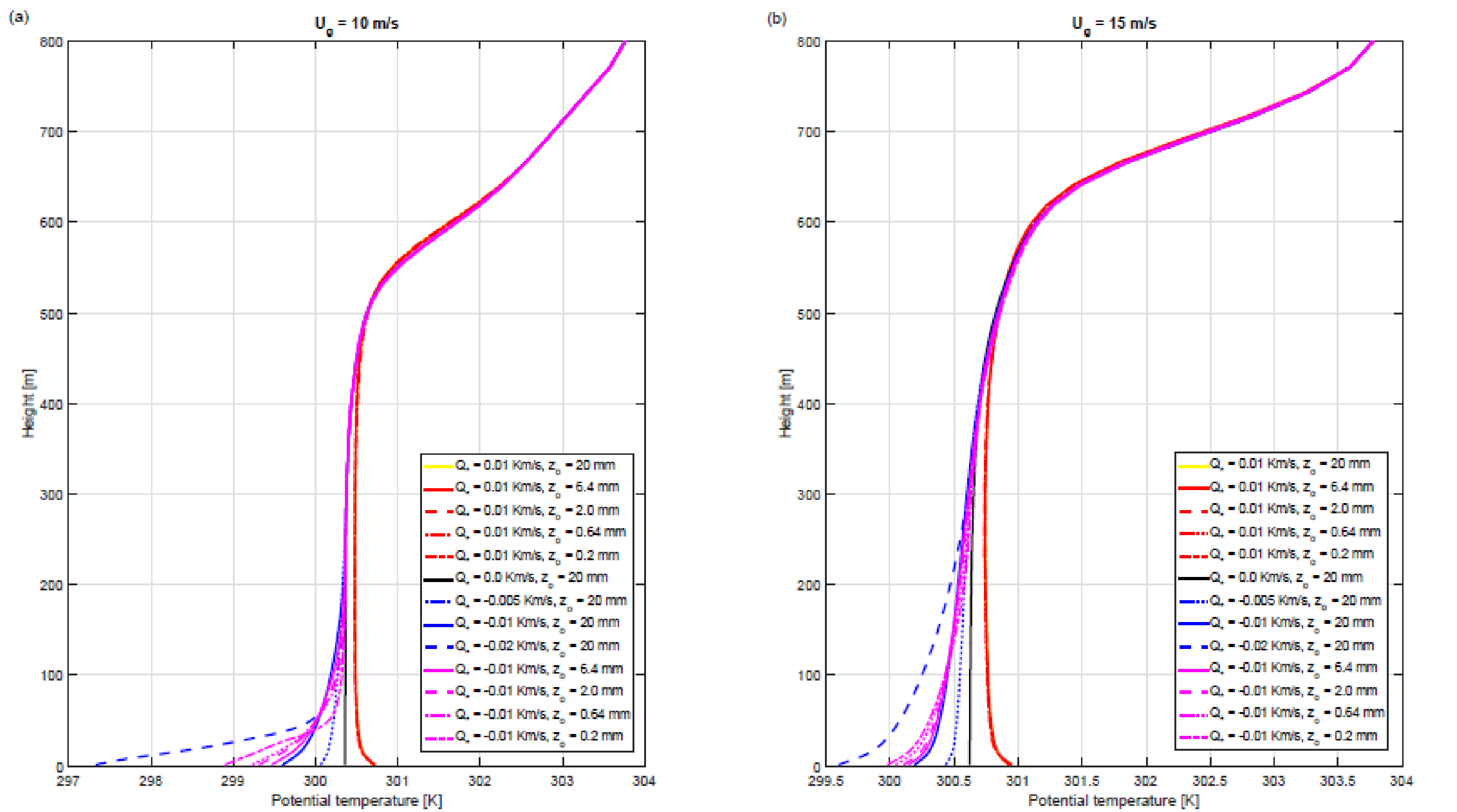

Figure 2. Vertical profile of potential temperature from last 30 min of the simulations.

Table 1. Details of the ABL conditions analyzed for the last 30 min of each simulation. Global parameters are shown for simulations of convective (C), neutral (N) and stable (S) conditions. The geostrophic wind speed is indicated from the simulation name as U10 or U15 denoting 10 or 15 m/s wind speed. Changes in surface roughness z_0 is indicated (Z) or if no change is made relative to initial state we name it reference run (R).

Case Unit	U_g $[ms^{-1}]$	Q_* $[Kms^{-1}]$	z_0 $[mm]$	u_* $[ms^{-1}]$	$z_{i(UW)}/L$ -	$z_{i(UW)}$ $[m]$	$z_{i(TKE)}$ $[m]$	$z_{i(WT)}$ $[m]$	$z_{i(d\theta/dz)}$ $[m]$
CU10R1	10	0.01	20.0	0.36	-1.61	563	591	519	44
CU10Z2	10	0.01	6.4	0.33	-2.04	552	572	501	44
CU10Z3	10	0.01	2.0	0.31	-2.62	571	590	523	46
CU10Z4	10	0.01	0.64	0.28	-3.10	534	568	502	44
CU10Z5	10	0.01	0.20	0.26	-3.88	531	435	518	40
NU10R1	10	0.00	20.0	0.30	0.00	328	254	550	1
SU10R1	10	-0.005	20.0	0.27	0.79	239	167	553	76
SU10R2	10	-0.01	20.0	0.23	1.84	174	114	553	187
SU10R3	10	-0.02	20.0	0.13	4.79	38	5	560	137
SU10Z1	10	-0.01	6.4	0.20	2.14	136	82	554	162
SU10Z2	10	-0.01	2.0	0.18	2.09	85	38	558	140
SU10Z3	10	-0.01	0.64	0.17	2.13	73	27	551	124
SU10Z4	10	-0.01	0.20	0.13	1.78	30	4	554	101
CU15R1	15	0.01	20.0	0.48	-0.81	663	697	561	38
CU15Z2	15	0.01	6.4	0.44	-0.98	646	691	576	40
CU15Z3	15	0.01	2.0	0.42	-1.17	644	691	561	38
CU15Z4	15	0.01	0.64	0.39	-1.48	648	693	564	40
CU15Z5	15	0.01	0.20	0.36	-1.81	646	691	584	41
NU15R1	15	0.00	20.0	0.43	0.00	553	530	521	1
SU15R1	15	-0.005	20.0	0.42	0.45	515	431	599	30
SU15R2	15	-0.01	20.0	0.39	0.86	397	345	643	108
SU15R3	15	-0.02	20.0	0.36	1.75	302	253	642	321
SU15Z1	15	-0.01	6.4	0.36	0.92	327	265	637	147
SU15Z2	15	-0.01	2.0	0.33	1.07	305	234	634	167
SU15Z3	15	-0.01	0.64	0.31	1.20	261	187	646	203
SU15Z4	15	-0.01	0.20	0.28	1.31	224	155	646	199